Numerical Simulation of Dilute Turbulent Gas-Particle Flow with Turbulence Modulation

Akhil Rao and Jennifer S. Curtis
Dept. of Chemical Engineering, University of Florida, Gainesville, FL 32611

Bruno C. Hancock
Pfizer Global Research and Development, Groton, CT 06340

Carl Wassgren
School of Mechanical Engineering, Purdue University, West Lafayette, IN 47907

DOI 10.1002/aic.12673
Published online May 31, 2011 in Wiley Online Library (wileyonlinelibrary.com).

A numerical study of a dilute turbulent gas-particle flow with inelastic collisions and turbulence modulation in an Eulerian framework is described. A new interpretation is provided for the interaction/coupling terms, based on a fluctuating energy transfer mechanism. This interpretation provides for a new robust closure model for the interaction terms with the ability to predict the turbulence dampening as well as the turbulence enhancement phenomenon. Further, the model developed herein is investigated along with a variety of other published closure models used for the interaction/coupling terms, particle drag, and solid stress. The models are evaluated against several sets of benchmark experiments for fully-developed, turbulent gas-solid flow in a vertical pipe. © 2011 American Institute of Chemical Engineers *AIChE J,* 58: 1381–1396, 2012

Keywords: gas-solid flow, turbulence modulation, kinetic theory of granular flow

Introduction

Turbulent gas-solid flows are encountered in a large number of industrial applications such as pneumatic transport of powders, pulverized coal injection into entrained flow gasifiers, cyclones, and circulating fluidized beds. Modeling gas-solid flows is essential for designing and optimizing the processes involving such flows.

Louge et al.[1] developed an Eulerain two-fluid model for dilute turbulent gas-solid flow with particle–particle interactions. They were the first to use a single k-equation model to describe gas-phase turbulence. This model was further developed by Bolio et al.[2] who employed a two-equation k-ε model to describe the gas-phase turbulence. Simonin[3] and Benavides and van Wachem[4] have suggested models along similar lines. All these models are able to describe the mean velocity profiles of the gas and solid velocities well.

The granular temperature behavior for particles with low particle Reynolds numbers ($Re_p \sim 10$, Re_p is based on particle diameter and slip velocity) is also captured fairly well by these models, with some deviations from the experimental data of Tsuji (Tsuji, personal communication) for 243 μm polystyrene beads. According to these data, as the mass loading (ratio of the solid mass flux to the fluid mass flux, m) increases, the granular temperature decreases. Furthermore, for smaller mass loadings ($m \sim 1$) the granular temperature is virtually independent of the radial position, while for larger loadings ($m \sim 3$–5) the granular temperature increases towards the wall. This behavior suggests that for larger loadings (but still dilute-phase flow), particles tend to concentrate at the center of the pipe. These trends are correctly predicted by the models. Unfortunately, granular temperature data for large and intermediate Re_p are not available in the literature.

Correspondence concerning this article should be addressed to A. Rao at akhil-rao@hotmail.com.

In contrast, all of these models under predict the gas-phase turbulence in the presence of the particles. In fact, these models also predict that large particles ($d > 400$ μm) exhibit turbulence dampening, contrary to experimental observations as summarized by Gore and Crowe.[5] Hestroni[6] also showed that particles with small Re_p ($\sim$10) exhibit turbulence dampening, while particles with large Re_p ($\sim$1000) cause turbulence enhancement of the gas phase due to vortex shedding. Particles with intermediate Re_p ($\sim$100) show in-between behavior, exhibiting turbulence enhancement at the core of the pipe and turbulence dampening at the wall. This study further advances the work of Bolio et al.[2] and corrects for the deficiencies in these other gas-solid flow models.

To generate reliable predictions for gas-solid flow in an Eulerian framework, it is critically important to have accurate closure models. In particular, the gas-particle turbulent interactions, the effect of the presence of particles on gas-phase turbulence and vice versa, must be appropriately described. For state-of-the-art Eulerian, dilute gas-solid flow models with particle-particle interactions, there are several important forces/interactions requiring constitutive modeling. The flow models vary from one another in the following key aspects:

(1) the fluctuating interaction/coupling terms in the gas-phase turbulent kinetic energy and granular temperature equations which includes the gas-solid fluctuating velocity cross-correlation,

(2) the drag model, and

(3) the solid-phase stress model.

Although these closure models have evolved over time, there is no Eulerain model for dilute, turbulent gas-solid model flow with particle–particle interactions that is generally accepted.

Background

Fluctuating interaction terms

Louge et al.[1] suggested an approximation for closing the fluctuating interaction term. The fluctuating interaction term they proposed was based on the gas turbulence, granular temperature, and the gas-solid velocity cross-correlation. Time and volume based averaging (TVBA) was used for developing expressions for the fluctuating interactions. Louge et al.[1] closed the gas-solid velocity cross-correlation modifying Koch,[7] in which it is assumed that a dilute gas-solid suspension at very small particle Reynolds number in the limit where solid body collisions determine the particle velocity distribution function. TVBA and the modified Koch[7] gas-solid velocity cross-correlation were also used by Bolio et al.[2] and then tested by Benavides and van Wachem.[4] Along similar lines, Igci et al.[8] used a cross-correlation expression developed by Koch and Sangani,[9] but Igci et al.[8] neglected gas-phase turbulence in their analysis. More recently, Hadinoto and Curtis[10] used TVBA for the interaction term and applied a closure model for the gas-solid velocity cross-correlation developed by Wylie et al.[11] for particles with high inertia and moderate fluid inertia. Both the Koch and Sangani[9] and Wylie et al.[11] closure models are extensions of the original Koch[7] model, wherein the most important assumption is that the inertia of the fluid is negligible and the solid particle interactions occur for particles in viscous fluids with small particle Reynolds number. Bolio et al.,[2] Benavides and van Wachem[4] and Hadinoto and Curtis[10] observed that the aforementioned closure models could not predict the phenomenon of turbulence enhancement and under predicted the gas-phase turbulence in the presence of particles.

A closure model for the gas-solid velocity cross-correlation based on time scales was developed by Simonin[3] which is discussed later (in the Mathematical Model section). He too used TVBA to develop closure models to describe these fluctuating interaction terms. The NETL-MFIX code (Multiphase Flows with Interphase Exchanges) employs Simonin[3] closure model to simulate dilute, turbulent gas-solid phase flow. Benavides and van Wachem[4] have also tested the Simonin[3] closure. Predictions from the MFIX code as well as the work of Benavides and van Wachem[4] showed that the Simonin[3] model cannot predict the phenomenon of turbulence enhancement and under predicts the gas-phase turbulence in presence of particles.

Benavides and van Wachem[4] and Hadinoto and Curtis[10] also test a simple closure model for the gas-solid velocity cross-correlation developed by Sinclair and Mallo.[12] This model assumes the fluid—solid fluctuation velocity cross-correlation to be a geometric mean of the gas-phase turbulence and the granular temperature.

Finally, Crowe[13] developed a different form for the fluctuating interaction term. The Crowe[13] form includes additional generation based on the square of the relative velocity between the two phases. Volume based averaging (VBA) was used to develop new relations for the fluctuating interaction terms in contrast to most of the other models which have used TVBA to develop expressions for the fluctuating interaction terms. Only Zhang and Reese[14] have used the Crowe[13] formulation, along with a modified Koch and Sangani[9] model for the fluid-solid velocity cross-correlation, and observed a good match with available experimental data.

A new closure model for the fluctuating interactions is introduced in this study based on a fluctuating energy transfer mechanism analogous to a heat transfer mechanism. In this new closure, the Sinclair and Mallo[12] model is used for the gas-solid fluctuating velocity cross-correlation. Gas-solid flow predictions based on this closure compare more favorably to experimental data for gas turbulence and granular temperature than all of the previously published models. This new model is capable of predicting the gas-phase turbulence behavior associated with a wide range of particle sizes such as turbulence dampening in the presence of particles, turbulence enhancement, as well as in-between turbulence behavior.

Drag models

Wen and Yu[15] is probably the most widely used and accepted particle drag model. However, Hadinoto and Curtis[10] showed that the choice of the drag model may affect the predicted mean and fluctuating velocity profiles in dilute gas-solid flow for small and low density particles at low velocities. In this study, flow predictions employing the (1) Wen and Yu[15] drag model, based on experimental correlation, the (2) Hill et al.[16,17] drag model, based on theory and Lattice—Boltzman simulations, and the (3) Syamlal and O'Brien drag model,[18] also based on experimental correlation, are investigated and compared.

Table 1. Closure Relations Employed in the Published Gas Solid Flow Models

Model	Interaction Term (I_k, I_T)	Cross - Correlation (k_{sg})	Drag Force (F_D)	Solid Stress (μ_s, λ_s,)
Bolio et al.[2]	TVBA, Eqs. 4 and 5	Louge et al.[1]	Wen and Yu[15]	Lun et al.[19]
MFIX[3]	TVBA, Eqs. 4 and 5	Simonin[3]	Syamlal and O'Brien model[18]	Peirano and Leckner[20]
Zhang and Reese[14]	VBA,Crowe[13], Eqs. 14 and 15	Zhang and Reese[14]	Zhang and Reese[14]	Peirano and Leckner[20]
Benavides and van Wachem[4]	TVBA, Eqs. 4 and 5	Louge et. al.[1], Simonin[3], Sinclair and Mallo[12]	Wen and Yu[15]	Peirano and Leckner[20]
Present study	TVBA, Eqs. 4 and 5	Louge et al.,[1] Koch and Sangani[9], Wiely et al.,[11] Simonin[3], Sinclair and Mallo[12]	Wen and Yu[15], Syamlal and O'Brien model[18], Hill et al.[16,17]	Lun et al.,[19] Peirano and Leckner[20]
	VBA,Crowe[13], Eqs. 14 and 15	Zhang and Reese[14]		
	FET, Eqs. 25 and 26	Sinclair and Mallo[12]		
New proposed model	FET, Eqs. 25 and 26	Sinclair and Mallo[12]	Wen and Yu[15]	Peirano and Leckner[20]

TVBA, time and volume based averaging for I_k and I_T; VBA, volume based averaging for I_k and I_T; FET, I_k and I_T are based on the fluctuation energy transfer mechanism.

Solid-phase stress model

Two different closures for the solid-phase stress are considered in this study. Both of these originate from the kinetic theory for granular flow. The Lun et al.[19] granular flow theory was the first fundamental description for the solid-phase stress based on analogy with molecular collisions in a dense gas. The second model, based on the work of Peirano and Leckner,[20] includes the effect of gas-phase turbulence and the effect of the interstitial fluid in the description for the solid-phase stress.

Table 1 summarizes the closures used by the various dilute, turbulent gas-solid flow models in the literature. As outlined above, several model formulations obtained by combining the different interaction/coupling term formulations along with the various gas-solid velocity cross-correlations, three different drag force models, and two different solid-phase stress models, are compared and tested against benchmark experimental data provided by Tsuji et al.,[21] Jones et al.,[22] Sheen et al.,[23] and Lee and Durst.[24] These data sets were obtained under the conditions of fully-developed, dilute, turbulent gas-solid flow in a vertical pipe using laser Doppler velocimetry. The mean and fluctuating velocity profiles of the gas and solid phases have been reported in these experiments. After evaluating all the combinations of the models, Table 1 puts forth the final model which yields minimum errors when compared to the various data sets.

Mathematical Model

The continuum equations for an Eulerian description of dilute, turbulent gas-solid flow have been well documented in many studies. The two-fluid equations used in this work follow those given in Bolio et al.[2] Table 2 presents the Bolio et al.[2] governing equations for the simplified case of fully-developed, dilute, turbulent gas-solid flow in a vertical pipe of radius (R). These simplified equations are also consistent with the gas/solid turbulence model of Simonin implemented in MFIX[25] and Benavides and van Wachem.[4]

Fluid stress (τ_{rz})

The total fluid stress (τ_{rz}) has two components. First, there is the viscous fluid component in which the intrinsic gas viscosity (μ_g) is affected by the presence of the solid (Table 2, Fluid Stress). The effect on μ_g for very dilute solids concentration cases is given by Batchelor and Green.[26] The second component in the total fluid stress is the turbulent contribution (Reynold Stress) which is simplified using an eddy viscosity closure. For the two—equation k-ε turbulence model, the eddy viscosity is described based on the turbulent kinetic energy (k) and its dissipation rate (ε). The turbulence model coefficients (c_{T1}, c_{T2}, c_{T3}, c_μ, σ_k, σ_ε, f_{T1}, f_{T2}, and f_μ) are the same as given in Bolio et al.[2] and are summarized in Table 3.

Drag force ($\mathbf{F}_D$)

The drag force is proportional to the relative velocity and to the drag coefficient β, which is a function of the solids volume fraction (v), and particle Reynolds number. Table 4 provides the details for the three drag models considered in this study: Wen and Yu,[15] Hill et al.,[16,17] and Syamlal and O'Brien.[18] The Hill et al.[16,17] model is not directly extracted from the original papers but follows the equation set presented in Benyahia et al.[27]

Granular energy dissipation (γ), solid-phase stress (σ_{rz}, σ_{rr}, $\sigma_{\theta\theta}$), and granular energy flux ($\mathbf{q}_{pTr}$)

Granular energy is dissipated due to inelastic collisions of particles with a restitution coefficient (e). This granular energy dissipation is given by Lun et al.[19] and is a function of the radial distribution function (g_0), the solid volume fraction (v), and granular temperature (T).

The solid-phase stresses have two contributions: the kinetic (or translational) part (σ^k) and the collisional part (σ^c). Bolio et al.[2] modified the Lun et al.[19] stress expressions so that the kinetic contribution remains bounded in finite-sized domains and dampens according to a function ω proportional to the mean free path of the particles. Consequently

$$\sigma = \omega\sigma^k + \sigma^c \tag{1}$$

where

$$\omega = \frac{1}{1 + \lambda_{mfp}/R} \tag{2}$$

and the mean free path, λ_{mfp} is

$$\lambda_{mfp} = \frac{d}{6\sqrt{2}v} \tag{3}$$

The descriptions for the normal solid-phase stresses (σ_{rr}, $\sigma_{\theta\theta}$) are very similar in Lun et al.[19] and Peirano and Leckner,[20] with the primary difference being with the presence of the damping function ω in the Lun et al.[19] formulation. In this

Table 2. Fully Developed Gas-Solid Flow Model in Vertical Pipes

Gas phase momentum balance (z-component)

$$0 = \frac{1}{r}\frac{\partial}{\partial r}(r\tau_{rz}) - F_{Dz} - \frac{dp}{dz}$$

Solid phase momentum balance (z-component)

$$0 = -\frac{1}{r}\frac{\partial}{\partial r}(r\sigma_{rz}) + F_{Dz} + \rho_s v g$$

Solid phase momentum balance (r-component)

$$0 = \frac{1}{r}\frac{\partial}{\partial r}(r\sigma_{rr}) - \frac{\sigma_{\theta\theta}}{r}$$

Granular energy balance

$$0 = -\frac{1}{r}\frac{\partial}{\partial r}(rq_{PTr}) - \sigma_{rz}\frac{\partial V_{sz}}{\partial r} - \gamma + I_T$$

Transport equations for k-ε

$$0 = \frac{1}{r}\frac{\partial}{\partial r}\left[r(1-v)\left(\frac{\mu_{eg}}{\rho_g} + \frac{\mu_T}{\sigma_k \rho_g}\right)\frac{\partial k}{\partial r}\right] + (1-v)\frac{\mu_T}{\rho_g}\left(\frac{\partial V_{gz}}{\partial r}\right)^2 - (1-v)\varepsilon + I_k$$

$$0 = \frac{1}{r}\frac{\partial}{\partial r}\left[r(1-v)\left(\frac{\mu_{eg}}{\rho_g} + \frac{\mu_T}{\sigma_\varepsilon \rho_g}\right)\frac{\partial \varepsilon}{\partial r}\right] (1-v)c_{T1}f_{T1}\frac{\varepsilon}{k}\frac{\mu_T}{\rho_g}\left(\frac{\partial V_{gz}}{\partial r}\right)^2 (1-v)c_{T2}f_{T2}\frac{\varepsilon^2}{k} + (1-v)c_{T3}f_{T2}\frac{\varepsilon}{k}I_k$$

Fluid stress (τ_{rz})

$$\tau_{rz} = (\mu_{eg} + \mu_T)\frac{\partial V_{gz}}{\partial r}$$

Batchelor and Green[25]

$$\mu_{eg} = \mu_g(1 + 2.5v + 7.6v^2)\left(1 - \frac{v}{v_0}\right)$$

$$\mu_T = \frac{c_\mu f_\mu \rho_g k^2}{\varepsilon}$$

Drag force (F_D)

$$F_{Dz} = \beta(V_{gz} - V_{sz})$$

β is detailed in Table 4

Granular energy dissipation (γ)

$$\gamma = \frac{48}{\sqrt{\pi}}\eta(1-\eta)g_0 v^2 \frac{\rho_s}{d}T^{3/2}$$

where

$$T = \frac{1}{3}(\overline{v_{si}v_{si}}); \eta = \frac{(1+e)}{2}; g_0 = \frac{v_0^{1/3}}{v_0^{1/3} - v^{1/3}}$$

Solid-phase stress (σ_{rz}, σ_{rr}, $\sigma_{\theta\theta}$)

Normal stresses: $\sigma_{rr} = \sigma_{\theta\theta} = \rho_s(\omega G_{1k} + G_{1c})T$ (for Lun etal.[19])

Normal stresses: $\sigma_{rr} = \sigma_{\theta\theta} = \rho_s(G_{1k} + G_{1c})T$ (for Perino and Leckner,[20])

(*Continued*)

Table 2. (Continued)

where,

$$G_{1k} = v$$

$$G_{1c} = 4\eta v^2 g_0$$

Shear stress : $\sigma_{rz} = -\mu_s\frac{\partial V_{sz}}{\partial r}$

Granular energy flux (q_{pTr})

$$q_{pTr} = -\lambda\frac{\partial T}{\partial r}$$

study, the Bolio et al.[2] expressions have been followed for the normal solid stress when the Lun et al.[19] model is used.

The shear stress for the solid phase is expressed as a product of the solid-phase viscosity (μ_s) and the solid velocity strain (see Table 2, Solid-Phase Stress).

Similar to the solid-phase shear stress, the granular energy flux is expressed as a product of the granular (or pseudo-thermal) conductivity (λ), and the gradient of granular temperature (Table 2, Granular Energy Flux). The expressions for the solids viscosity (μ_s) and conductivity (λ) as given by Lun et al.[19] and Peirano and Leckner[20] are quite different and are detailed in Table 5. The Simonin[3] expressions have been followed for the solids viscosity (μ_s) and conductivity (λ) when the Peirano and Leckner[20] model is used.

Fluctuating interaction/coupling terms (I_k, I_T)

Louge et al.[1] used TVBA and simplified the fluctuating interaction/coupling terms to the following form

$$I_k = -\beta(1-v)\left(2k - \overline{v'_{gi}v'_{si}}\right) \quad (4)$$

$$I_T = \beta(1-v)\left(\overline{v'_{gi}v'_{si}} - 3T\right) \quad (5)$$

where I_k represents the interaction coupling between the granular temperature and the gas-phase turbulence equation and I_T is the interaction coupling between the gas-phase turbulence and the granular energy balance equation. For the sake of convenience, the cross-correlation of the gas and solid fluctuating velocities $\overline{v'_{gi}v'_{si}}$ will be denoted as k_{sg} hereafter.

The description for k_{sg} is probably the most controversial point amongst the different closures required for gas-solid

Table 3. Gas Turbulence Model

Bolio et al.[2]

$c_{T1} = 1.4$, $c_{T2} = 1.8$, $c_{T3} = 1.2$, $c_\mu = 0.09$, $\sigma_k = 1.4$, $\sigma_\varepsilon = 1.3$

$$f_{T1} = 1$$

$$f_{T2} = \left[1 - \frac{2}{9}\exp\left\{-\left(\frac{R_T}{6}\right)^2\right\}\right]\left[1 - \exp\left\{-\frac{y^+}{5}\right\}\right]^2$$

$$f_\mu = \left[1 - \exp\left(-\frac{y^+}{70}\right)\right]\left[1 + \frac{3.45}{\sqrt{R_T}}\right]$$

where,

$$y^+ = \frac{U_\tau \rho_g}{\mu_g}(R - r) \text{ and } R_T = \frac{\rho_g k^2}{\mu_{eg}\varepsilon}$$

Table 4. Drag Coefficient

Wen and Yu[15]

$$\beta = \frac{3}{4}\frac{\rho_g}{d} C_D \frac{v}{(1-v)^{2.65}} |V_{gz} - V_{sz}|$$

$$C_D = \frac{24}{Re_p}\left(1 + 0.15\, Re_p^{0.687}\right) \qquad \text{for } Re_p \le 1000$$

$$C_D = 0.44 \qquad \text{for } Re_p > 1000$$

$$Re_p = \frac{(1-v)\rho_g d|V_{gz} - V_{sz}|}{\mu_g}$$

Hill et al.[16,17] model

$$\beta = 18\mu_g(1-v)v\frac{F}{d^2}$$

$$F = 1 + \frac{3}{8} Re_p \qquad \text{for } v \le 0.01 \text{ and } Re_p \le \frac{F_2 - 1}{3/8 - F_3}$$

$$F = F_0 + F_1 Re_p^2 \qquad \text{for } v > 0.01 \text{ and } Re_p \le \frac{F_3 + \sqrt{F_3 - 4F_1(F_0 - F_2)}}{2F_1}$$

$$F = F_2 + F_3 Re_p \qquad \text{for } v \le 0.01 \text{ and } Re_p > \frac{F_2 - 1}{3/8 - F_3}$$

$$F = F_2 + F_3 Re_p \qquad \text{for } v > 0.01 \text{ and } Re_p > \frac{F_3 + \sqrt{F_3 - 4F_1(F_0 - F_2)}}{2F_1}$$

$$F_0 = (1 - w_{HLK})\left[\frac{1 + 3\sqrt{v/2} + (135/64)v\ln(v) + 17.14v}{1 + 0.681v - 8.48v^2 + 8.16v^3}\right] + w_{HLK}\left[10\frac{v}{(1-v)^3}\right] \qquad \text{for } v<0.4$$

$$F_1 = \frac{1}{40}\sqrt{\frac{2}{v}} \qquad \text{for } v<0.1$$

$$F_2 = (1 - w_{HLK})\left[\frac{1 + 3\sqrt{v/2} + (135/64)v\ln(v) + 17.89v}{1 + 0.681v - 11.03v^2 + 15.41v^3}\right] + w_{HLK}\left[10\frac{v}{(1-v)^3}\right] \qquad \text{for } v<0.4$$

$$F_3 = 0.9531v + 0.03667 \qquad \text{for } v<0.0953$$

$$w_{HKL} = \exp[-10(0.4 - v)/v]$$

$$Re_p = \frac{(1-v)\rho_g d|V_{gz} - V_{sz}|}{2\mu_g}$$

Syamlal and O'Brien[18]

$$\beta = \frac{3v\rho_g}{4V_{rm}^2 d}\left(0.63 + 4.8\sqrt{V_{rm}/Re_p}\right)^2 |V_{gz} - V_{sz}|$$

$$V_{rm} = 0.5\left(A - 0.06Re_p + \sqrt{(0.06Re_p)^2 + 0.12Re_p(2B_{SO} - A_{SO}) + A^2}\right)$$

$$A_{SO} = (1-v)^{4.14} \text{ and } B_{SO} = (1-v)^{2.65}$$

$$Re_p = \frac{\rho_g d|V_{gz} - V_{sz}|}{\mu_g}$$

flow modeling in an Eulerian framework. This controversy is due to the fact that there is a lack of fundamental understanding concerning the nature of the fluid-solid interactions at the level of the velocity fluctuations.

In the gas-solid flow model of Louge et al.,[1] the authors modified the expression of Koch[7] who rigorously derived k_{sg}. However, Koch[7] assumed the system to have negligible fluid inertia with particles suspended in a viscous fluid. Consequently, the Koch's[7] k_{sg} lacks the effect of gas-phase turbulence on the cross-correlation. Hence, the fluid-solid fluctuating interactions that have evolved from the Koch[7] model may not be appropriate in the case of turbulent gas-solid flow.

Igci et al.[8] employed the work of Koch and Sangani,[9] an extension of the Koch[7] model, in a system where the fluid turbulence was again neglected. Koch and Sangani[9] used a ψ factor to summarize the effect of the solids concentration. ψ replaces the solid volume fraction functionality obtained from using the drag term (β) in the work of Louge et al.[1] Hadinoto and Curtis[10] used another form of the Koch[7] model based on the work of Wylie et al.[11] This model included the effect of large particle inertia and moderate fluid inertia by enhancing the ψ factor with a functionality which depends on v, Re_T, and Re_p. Table 6 provides the details of the evolution of Koch's[7] gas-solid velocity cross-correlation.

Table 5. Solid Viscosity, μ_s, and Solid Conductivity, λ

Lun et al.[20] (as modified by Bolio et al.[2])

Solid viscosity

$$\mu_s = \mu_s^{'}(\omega G_{2k} + G_{2c})$$
$$\mu_s^{'} = \frac{5\sqrt{\pi}}{96}\rho_s d\sqrt{T}$$
$$G_{2k} = \frac{1}{\eta(2-\eta)g_0}\left[1 + \frac{8}{5}\eta v g_0(3\eta - 2)\right]$$
$$G_{2c} = \frac{8v}{5(2-\eta)}\left[1 + \frac{8}{5}\eta v g_0(3\eta - 2)\right] + \frac{768v^2 g_0 \eta}{25\pi}$$

Bulk Solid Viscosity

$$\mu_b = \frac{256\mu_s v^2 g_0}{5\pi}$$

Solid Conductivity

$$\lambda = \lambda'(\omega G_{3k} + G_{3c})$$
$$\lambda' = \frac{25\sqrt{\pi}}{128}\rho_s d\sqrt{T}$$
$$G_{3k} = \frac{8}{\eta(41-33\eta)g_0}\left[1 + \frac{12}{5}\eta^2 v g_0(4\eta - 3)\right]$$
$$G_{3c} = \frac{96v}{5(41-33\eta)}\left[1 + \frac{12}{5}\eta^2 v g_0(4\eta - 3) + \frac{16}{5\pi}\eta v g_0(41\eta - 33)\right]$$

Peirano and Leckner[20]

Solid Viscosity

$$\mu_s = v\rho_s(G_{2k} + G_{2c})$$
$$G_{2k} = \left[\frac{2}{3}k_{sg}\eta_t + T(1 + A_{PL} v g_0)\right]\left(\frac{2}{\tau_D} + \frac{B_{PL}}{\tau_c}\right)^{-1}$$
$$G_{2c} = \frac{8}{5}v g_0 \eta\left(G_{2k} + d\sqrt{\frac{T}{\pi}}\right)$$

Bulk Solid Viscosity

$$\mu_b = \frac{5}{3}v\rho_s G_{2c}$$

Solid Conductivity

$$\lambda = v\rho_s(G_{3k} + G_{3c})$$
$$G_{3k} = \left[\frac{9}{10}k_{sg}\eta_t + \frac{3}{2}T(1 + C_{PL} v g_0)\right]\left(\frac{9/5}{\tau_D} + \frac{D_{PL}}{\tau_c}\right)^{-1}$$
$$G_{3c} = \frac{18}{5}v g_0 \eta\left(G_{3k} + \frac{5}{9}d\sqrt{\frac{T}{\pi}}\right)$$
$$A_{PL} = 2/5(1+e)(3e-1)$$
$$B_{PL} = (1+e)(3-e)/5$$
$$C_{PL} = (1+e)^2(2e-1)/100$$
$$D_{PL} = (1+e)(49-33e)/100$$

Simonin[3] developed a model for the gas-solid fluctuation velocity cross-correlation based on the Lagrangian time scale and particle relaxation time scale. The Lagrangian time is the large-eddy time scale as felt by crossing particles and is defined as

$$\tau_L = \frac{\tau_e}{\sqrt{1 + c_\beta \xi_r^2}} \tag{6}$$

where the eddy time scale (τ_e, the turn over time of an eddy) is defined as

$$\tau_e = \frac{3}{2}c_\mu f_\mu \frac{k}{\varepsilon} \tag{7}$$

and

$$\xi_r^2 = \frac{3\left|V_g - V_s\right|^2}{2k} \tag{8}$$

$$c_\beta = 1.8 - 1.35\cos^2(\theta') \tag{9}$$

The parameter θ' is the angle between the mean fluid and solid velocity vectors. The particle relaxation or the drag time (τ_D) is the time for which the effect of a passing particle can be felt on the neighboring fluid

$$\tau_D = \frac{v\rho_s}{\beta(1-v)} \tag{10}$$

The Simonin model assumes that the ratio of the Lagrangian time scale (τ_L) to the particle relaxation time (τ_D) is equal to the ratio of the fluctuation energy of the cross-correlation carried by the gas phase to the fluctuation energy carried by the entire mixture. That is

$$\eta_t = \frac{\tau_L}{\tau_D} = \frac{\rho_g v_g k_{sg}}{\left(2\rho_g v_g k + 3\rho_s v_s T - \rho_{avg} k_{sg}\right)} \tag{11}$$

Equation 11 on rearrangement gives

$$k_{sg} = \frac{\eta_t}{1 + [1+\chi]\eta_t}[2k + 3\chi T] \tag{12}$$

where

Table 6. Gas Solid Velocity Cross Correlations which have Evolved from Koch[7]

Koch[7] expression as modified by Louge et al.,[1]

$$k_{sg} = \frac{4}{\sqrt{\pi}}\frac{d}{\rho_s}\frac{\beta(1-v)}{v}\frac{\left(V_{gz} - V_{sz}\right)^2}{\sqrt{T}}$$

Koch and Sangani[9] expression as used by Igci et al.,[8]

$$\beta(1-v)k_{sg} = \frac{81 v\mu_g^2\left|V_{gz} - V_{sz}\right|^2}{g_0 d^3 \rho_g \sqrt{\pi T}}\psi$$

where

$$\psi = \frac{\left(1 + 3\sqrt{v/2} + (135/64)v\ln(v) + 17.14v\right)^2}{(1 + 3.5\sqrt{v} + 5.9v)(1 + 0.681v - 8.48v^2 + 8.16v^3)^2}$$

Wylie et al.[11] expression as used by Hadinoto and Curtis,[10]

$$\beta(1-v)k_{sg} = \frac{81 v\mu_g^2\left|V_{gz} - V_{sz}\right|^2}{g_0 d^3 \rho_g \sqrt{\pi T}}\psi'$$

where

$$\psi' = \psi + K_{fb} Re_p \psi''$$
$$K_{fb} = 0.0336 + 0.106v + 0.0116(1-v)^{-5}$$
$$\psi'' = \left(1 + 2\frac{Re_T^2}{Re_p^2} - \frac{Re_T^4}{Re_p^4}\right)\mathrm{erf}\left(\frac{Re_T}{\sqrt{2}Re_p}\right) + \sqrt{\frac{2}{\pi}}\frac{Re_T}{Re_p}\left(1 + \frac{Re_T^2}{Re_p^2}\right)\exp\left(-\frac{Re_d^2}{2Re_p^2}\right)$$
$$Re_p = \frac{\rho_g d\left|V_{gz} - V_{sz}\right|}{\mu_g}$$
$$Re_T = \frac{\rho_g d\sqrt{T}}{\mu_g}$$

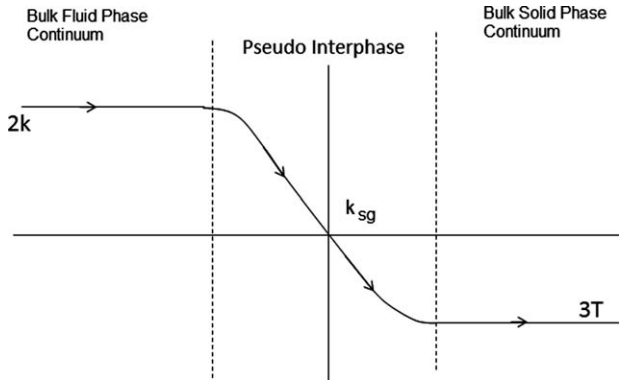

Figure 1. Profile for the fluctuating energy transfer.

$$\chi = \frac{\rho_s v}{\rho_g (1 - v)} \tag{13}$$

Benviades and van Wachen,[4] and Benyahia et al.[30] also use Eq. 12 while using the Simonin model for the velocity cross-correlation closure.

Crowe[13] argued that it was incorrect to take the averaged flow variables as being local flow variables and to treat the governing equations as if they represented single-phase flow with a local coupling term. Hence, Crowe[13] suggested a new approach for the development of the governing equations which is not based on temporal and volume averaging, but is based on volume averaging only (VBA). The equations he used for the fluctuation interaction terms I_k and I_T, are different than those normally used by others

$$I_k = \beta(1 - v)\left|V_g - V_s\right|^2 + \beta(1 - v)\left(3T - k_{sg}\right) \tag{14}$$

$$I_T = \beta(1 - v)\left(k_{sg} - 3T\right) \tag{15}$$

In this formulation, the first term in Eq. 14 reflects the conservation of mechanical work by drag force into turbulence kinetic energy. The second term in Eq. 14 is a redistribution term representing the transfer of kinetic energy of particle motion to the kinetic energy of the carrier fluid. The additional generation term which is proportional to the square of the relative velocity between the two phases (Eq. 14), arising due to the new averaging technique. This additional generation helps in predict enhanced fluid turbulence. The model of Zhang and Reese[14] employs Eqs. 14 and 15 for the fluctuating interaction terms along with a modified Koch and Sangani[9] model to describe the cross-correlation between the fluid and solid fluctuating velocity

$$k_{sg} = \left|V_g - V_s\right|^2 \frac{\tau_c}{\tau_D} \tag{16}$$

where the collision time τ_c is the time between collisions and is defined as

$$\tau_c = \frac{d}{24 v g_0} \sqrt{\frac{\pi}{T}} \tag{17}$$

Zhang and Reese[14] showed good predictions when compared with the Tsuji et al.[21] data. Sinclair and Mallo[12] developed a simple model for the cross-correlation of fluid-solid velocity fluctuations using a simple geometric mean

$$k_{sg} = \sqrt{6kT} \tag{18}$$

Equation 18 is obtained by assuming that the correlation of the fluctuating gas velocity and the fluctuating drag force ($\overline{v'_{gi} f_{Di}}$) divided by the gas fluctuation velocity is equal to the correlation of the fluctuating solid velocity and the fluctuating drag force ($\overline{v'_{si} f_{Di}}$) divided by the fluctuating solid velocity, i.e.

$$\frac{\overline{v'_{gi} f_{Di}}}{\left(\overline{v'_{gi} . v'_{gi}}\right)^{1/2}} \cong -\frac{\overline{v'_{si} f_{Di}}}{\left(\overline{v'_{si} . v'_{si}}\right)^{1/2}} \tag{19}$$

where f_{Di} is the fluctuating drag force. The correlation between fluctuating gas velocity and the fluctuating drag force is generally approximated as I_k, the effect of solids on the gas turbulence, and the correlation of fluctuating solid velocity and the fluctuating drag force is approximated as I_T, the effect of gas turbulence on the granular temperature. Thus Eq. 19 can be interpreted as

$$\frac{I_k}{\sqrt{2k}} = -\frac{I_T}{\sqrt{3T}} \tag{20}$$

Substituting Eqs. 4 and 5 into Eq. 20 gives

$$\frac{\beta\left(2k - k_{sg}\right)}{\sqrt{2k}} = \frac{\beta\left(k_{sg} - 3T\right)}{\sqrt{3T}} \tag{21}$$

Equation 21 on simplification gives Eq. 18.

New fluctuating energy transfer (FET) model for the fluctuating interaction/coupling terms

To develop the new fluctuating interaction model (FET model), we consider the hypothetical situation where:

(1) Particles are enclosed and suspended freely in a box with no gravitational acceleration.

(2) The fluid has negligible viscosity; hence, there is no momentum diffusion and no turbulence dissipation.

(3) The collisions of the particles are elastic; consequently, there is no dissipation due to collisions.

(4) The diffusion of particle momentum is also negligible.

(5) There are no wall effects.

Now, assume that at the start of an experiment the particles are stationary but the gas has an evenly distributed turbulent energy given by k. In this situation, the gas-phase turbulence will initiate some velocity fluctuations in the particle phase that will continue to grow. In this hypothetical situation, the gas-phase turbulent kinetic energy and granular energy equations will reduce to

$$\rho_g (1 - v)\frac{\partial k}{\partial t} = -I_k = -\beta'(1 - v)\left(2k - k_{sg}\right) \tag{22}$$

$$\frac{3}{2}\rho_s v \frac{\partial T}{\partial t} = I_T = \beta'(1 - v)\left(k_{sg} - 3T\right) \tag{23}$$

Equations 22 and 23 are analogous to the case of simple heat transfer between two immiscible fluids. The interaction terms are similar to convection heat transfer where ($2k - k_{sg}$) and ($k_{sg} - 3T$) are analogous to temperature differences

Table 7. Wake Term E_w

Lun[28]

$$E_w = 12\frac{C_w \mu_t k}{d^2}$$

$$Re_p = \frac{\rho_g d|V_{gz} - V_{sz}|}{\mu_g}$$

$\mu_t = 0.017 Re_p \mu_g$ for $150 \le Re_p < 310$

$\mu_t = 1.2 + 0.00005 Re_p^2 \mu_g$ for $310 \le Re_p < 610$

$\mu_t = 0.029 Re_p \mu_g$ for $Re_p \ge 610$

$C_w = 10/3$ for $150 \le Re_p < 310$

$C_w = 24/3$ for $Re_p \ge 310$

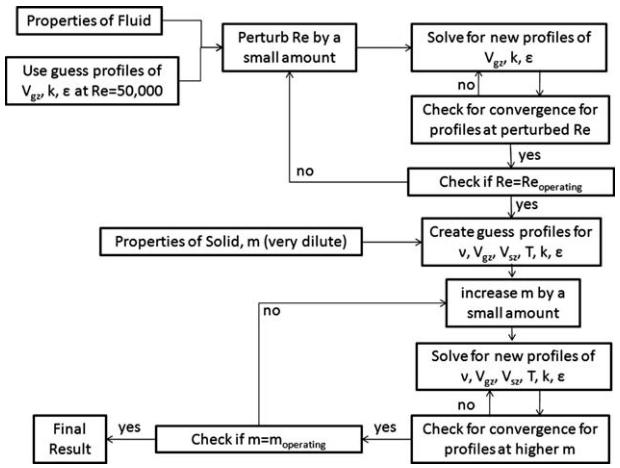

Figure 2. Program flow chart.

($T_{f1} - T_{f12}$) and ($T_{f12} - T_{f2}$), respectively (T_{f1} and T_{f2} are the bulk temperatures of the two fluids and T_{f12} is the temperature at the interface), and $\beta'(1-v)$ is analogous to the heat transfer coefficient multiplied by the surface area (hA_{ht}). For the defined hypothetical situation, the energy lost by the gas phase is equal to the energy gained by the solid phase

$$\frac{3}{2}\rho_s v \frac{\partial T}{\partial t} = -\rho_g (1-v)\frac{\partial k}{\partial t} \tag{24}$$

Figure 1 shows how the difference in the magnitude of the velocity fluctuations causes a transfer of energy from one phase to another, similar to the transfer of heat from one fluid phase to another. This picture of the energy transfer is consistent with the assumption of interpenetrating continua of the two phases and the use of the two-fluid model. The energy exchange will continue until the fluctuations equalize, that is, $k_{sg} = 2k = 3T$.

Typical units of $\beta'(1-v)$ are $M^1L^{-3}T^{-1}$ and so $\frac{\rho_g}{\beta'(1-v)}$ is a time scale (τ_{sg}) over which the transfer of fluctuation energy occurs. For particles with low inertia, that is, particles exhibiting turbulence dampening, the time scale for fluctuation energy transfer is τ_D. This behavior occurs because, for particles exhibiting turbulence dampening, the mechanism of the fluid being pulled along by the particles causes the transfer of fluctuation energy. Hence the drag time scale is the time over which the transfer of energy occurs. On the other hand, particles with higher inertia, that is, particles showing in-between behavior and turbulence enhancement, the time scale for fluctuation energy transfer is τ_c. For these particles, as they collide with each other and the wall, individual solid particles change their direction of flow. The change in direction of the particles causes a corresponding change in direction of the wake. The continuous changes in direction of the wakes, for these high inertia particles, cause an enhancement in the gas-phase turbulence. The collision time scale is time between which the particles and its wake changes direction and so the energy transfer occurs over the collisional time scale (τ_c) for the high inertia particles.

Finally, to describe the vortex shedding phenomenon associated with gas-phase turbulent enhancement, the fluctuating interaction/coupling term, I_k (Eq. 4), is enhanced by the wake effect E_w as given by Lun[28](Table 7). The coefficient C_w is slightly modified from what was originally prescribed in Lun[28] to produce a better fit to the experimental data. Thus, the following equations represent the complete fluctuating interaction/coupling terms for the new model

$$I_k = -\frac{\rho_g}{\tau_{sg}}(2k - k_{sg}) + E_w \tag{25}$$

$$I_T = \frac{\rho_g}{\tau_{sg}}(k_{sg} - 3T) \tag{26}$$

where τ_{sg} is the time scale for the fluctuation energy transfer ($\tau_{sg} = \tau_D$, for particles which show turbulence damping and τ_{sg}

Table 8. Summary of Experimental Data

Data	Size (μm)	Density (kg/m^3)	Mass Loading Cases 1	2	3	V_{gz} at r=0 (m/s) Cases 1	2	3	R (mm)	e,e_w,Φ	Profiles Provided
Tsuji et al.[21]	243	1020	0.5	1.3	3.2	13.1	12.8	10.8	15.25	0.9, 0.9, 0.002	V_{gz}, v_{gz}', v_{sz}'
	500	1020	0.7	1.3	3.4	12.2	13.3	10.7			V_{gz}, v_{gz}'
	1420	1030	0.6	2	2	13.4	12.8	13.2			V_{gz}, v_{gz}'
	2780	1020	0.6	2.3	3.4	14.5	13.8	14.2			V_{gz}, v_{gz}'
Jones[32]	70	2529	1	2	4	18.1	17.6	16.5	7.112	0.94, 0.94, 0.002	V_{gz}, V_{sz}, k, v_{sz}'
Lee and Durst[22]	400	2500		1.5			5.77		20.9	0.94, 0.94, 0.002	V_{gz}, V_{sz}
	100	2500		1.21			5.7				
Sheen et al.[23]	275	1020		1.224			8.785		26	0.9, 0.9, 0.002	V_{gz}, V_{sz}, v_{gz}'
	450	1020		0.885			9.22				V_{gz}, V_{sz}, v_{gz}'
	800	1020		1.5			9.686				V_{gz}, V_{sz}, v_{gz}'

For all cases, $\mu_g = 1.8 \times 10^{-5}$ Ns/m^2, $\rho_g = 1.2$ kg/m^3, and $v_0 = 0.65$.

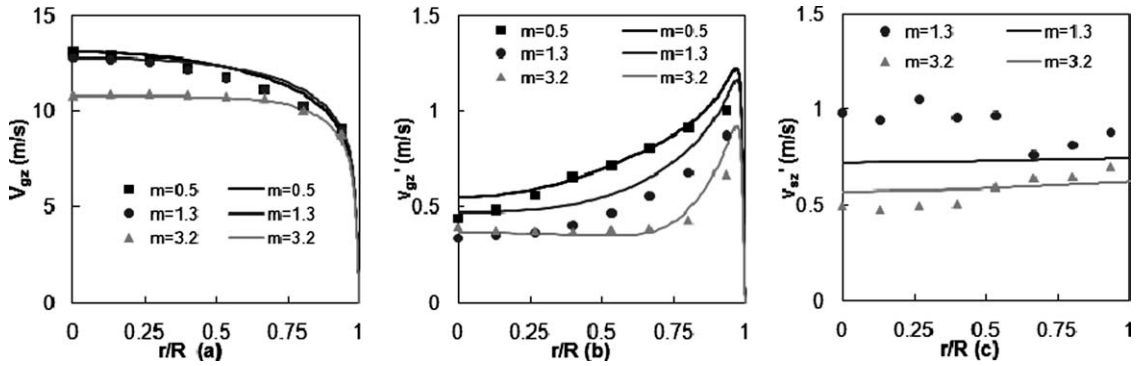

Figure 3. Present model predictions compared to Tsuji et al.[21] 243 μm particles.

$= \tau_c$, for particles which show in-between behavior and turbulence enhancement).

A couple of observations can be made about the cross-correlation k_{sg}:

(1) According to the new model and from the heat transfer analogy, k_{sg} must lie between $2k$ and $3T$.

(2) At the wall, as the instantaneous fluid velocity becomes zero due to the no-slip condition, the cross-correlation k_{sg} must also become zero.

Keeping these two conditions in mind, the Sinclair and Mallo[12] (Eq. 18) model is used for the cross-correlation k_{sg} since it is the only closure that is consistent with both conditions.

Boundary and operating conditions

Appropriate boundary conditions are also of prime importance to generate reliable flow predictions. At the center of the pipe, the symmetry boundary condition is used for all the flow variables. For the solid phase, boundary conditions at the wall for shear stress (σ_{rz}) and the flux of granular energy (q_{pT}) follow Johnson and Jackson.[29]

For the fluid phase at the wall, two sets of conditions were employed in this study. The first set of conditions is based on a low Reynolds number k-ε turbulence model as used by Bolio et al.[2] where turbulent transport equations for the fluid phase are integrated to the wall. For low Reynolds number k-ε turbulence model the mean and fluctuating fluid velocities are zero (no-slip boundary condition). Dissipation of gas turbulence at the wall is given by

$$\rho_g \varepsilon = \mu_{eg} \frac{\partial^2 k}{\partial r^2} + I_k \tag{27}$$

The second set of boundary conditions for the fluid phase employ wall functions for the fluid phase and follow the MFIX code.[30] These conditions assume some fluid velocity slip at the wall. Also, the wall conditions for k and ε are modified to be consistent with this approximation. The wall functions for the fluid-phase were used only when the code was being validated against the MFIX code and the results of Benavides and van Wachem.[4] For all the figures and tables in this study, the low Reynolds number k-ε turbulence model is used (i.e., no-slip boundary condition along with Eq. 27).

Numerical solution

To solve the governing equations numerically, one operating condition for the fluid phase and one for the solid phase are required. In the code developed for this study, two options are available for the operating condition on the fluid phase: the centerline fluid velocity or the fluid flow rate. The choice of which to use is made based on the conditions specified in the experimental data. For the solid phase, solid mass loading m is used to specify the operating condition. The solid loading m is defined as

$$m = \frac{\int \rho_s \nu V_{sz} r dr}{\int \rho_g (1-\nu) V_{gz} r dr} \tag{28}$$

The governing equations including the closure models, boundary and operating conditions are solved using a

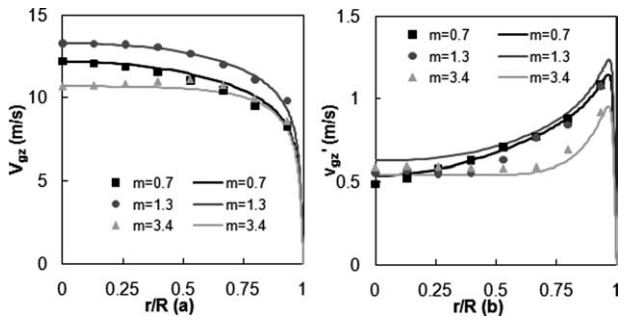

Figure 4. Present model predictions compared to Tsuji et al.[21] 500 μm particles.

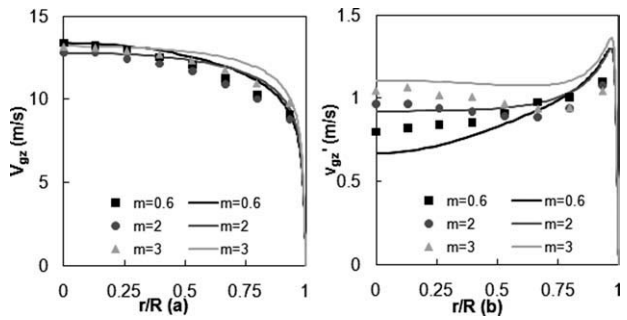

Figure 5. Present model predictions compared to Tsuji et al.[21] 1420 μm particles.

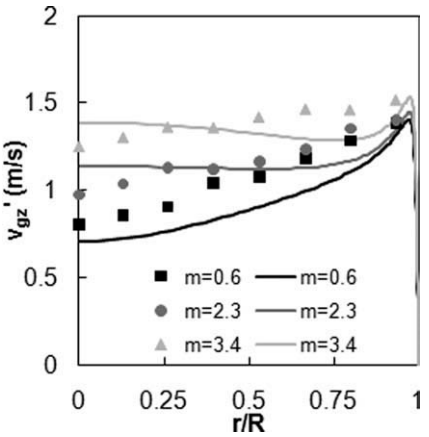

Figure 6. Present model predictions compared to Tsuji et al.[21] 2780 μm particles.

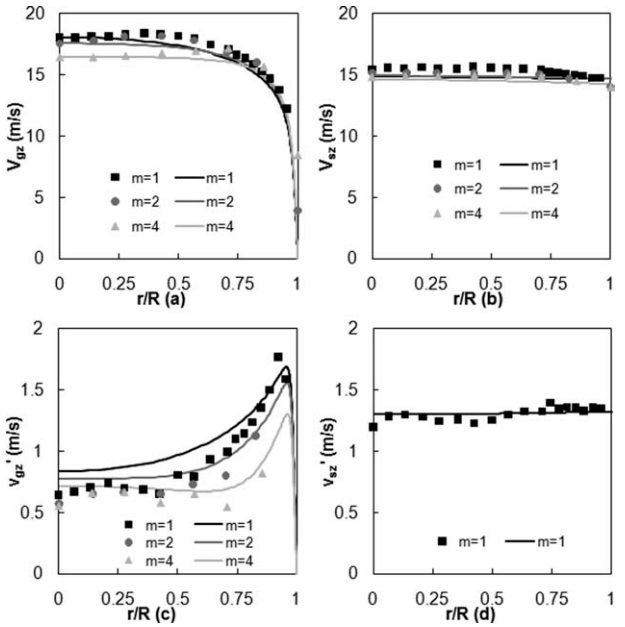

Figure 7. Present model predictions compared to Jones et al.[22] 70 μm particles.

combination of marching and iterative schemes as described in the following paragraph.

The continuum equations are discretized using the finite volume method approach described in Patankar and Spadling.[31] Approximately 100 discrete grid points were distributed in a nonuniform pattern throughout the domain cross-section with higher grid resolution near the wall. Bolio et al.[2] showed that 60 grid points were sufficient to generate a grid-independent solution.

Figure 2 depicts the flow chart for the code. First, an estimate using the single phase dimensionless fluid velocity V_{gz}, gas turbulence k, and gas-phase dissipation ε at a specific Re of flow (where $Re = \frac{\rho_g V_{avg} 2R}{\mu_g}$) are given as input to the code. The code then perturbs the Re towards the direction of the desired operating velocity and generates the new single-phase profiles for the perturbed Re in an iterative scheme. The operating condition is solved along with the discretized version of the single-phase gas momentum equation. The operating condition provides an additional equation which allows the pressure drop ($\bigtriangledown p$) to be treated as an unknown parameter. Thus, a pressure drop guess is not needed. The perturbations in Re are made until the operating Re is achieved (i.e., the operating velocity is achieved). At this point, an assumption is made that the fluid profile at very low solids loading will match the single phase profiles. Further, the guessed profiles for v, V_{sz}, and T are considered to be independent of r (the radial co-ordinate). The single phase profiles along with the guesses for v, V_{sz}, and T are taken as guesses for the very dilute case of two-phase profiles.

Like the fluid operating condition, the solid operating condition is solved along with the solid phase momentum balance (r-component) equation for the solid volume fraction profiles. The simulated flow profiles are used as a guess for the very dilute case. The loading is increased in small discrete steps (profiles for each loading step were calculated in an iterative scheme) until the two-phase flow operating conditions are obtained. Thus, in this fashion, a stable numerical solution is obtained.

The code is written in a modular fashion so that it is simple to toggle amongst the various closure models and boundary conditions. Hence, the code developed herein has the ability to easily reproduce the predicted flow patterns given in Bolio et al.,[2] Benavides and van Wachem,[4] and MFIX[25] (following the work of Simonin[3]). Therefore, this code provides a useful tool to compare various dilute turbulent gas-solid models against the same

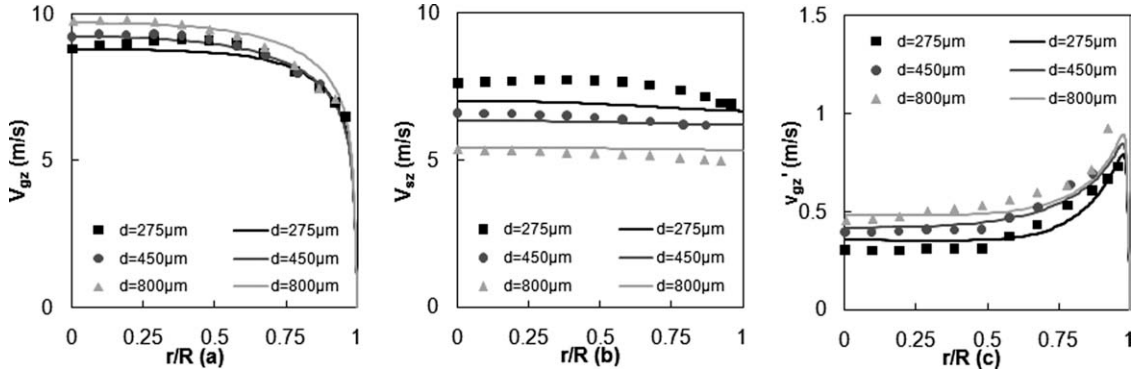

Figure 8. Present model predictions compared to Sheen et al.[23]

Table 9. Time Scale Used in FET Model for the Different Experimental Data

Experimental Data	Size (μm)	Density (kg/m^3)	~Re$_p$ No.	~Stokes No.	Time Scale Used	Vortex Shedding
Tsuji et al.[21]	243	1020	45	75	τ_D	No
	500	1020	130	320	τ_c	No
	1420	1030	730	2700	τ_c	Yes
	2780	1020	1800	11300	τ_c	Yes
Jones[32]	70	2529	12	50	τ_D	No
Lee and Durst[22]	400	2500	90	170	τ_c	No
	100	2500	5	12	τ_c	No
Sheen et al.[23]	275	1020	30	40	τ_D	No
	450	1020	85	115	τ_c	No
	800	1020	220	380	τ_c	Yes

benchmark experimental data sets on the same platform. Unfortunately, the code is unable to reproduce the results of Zhang and Reese[14] even after consultation with the authors.

Benchmark data sets

As stated earlier, the data under consideration are for pneumatic transport of solids by gas (air) in a vertical pipe. These flows are dilute and turbulent, and the flow profiles are fully developed. The data sets of Tsuji et al.,[21] Jones et al.,[22] Lee and Durst,[24] and Sheen et al.[23] span various sizes of polystyrene and glass bead particles (70–3000 μm) with Re approximately between 10,000 and 30,000 and mass loadings varying between 0 to 5. For succinctness, only the profiles obtained from what was found to be the most robust model, i.e., the model yielding the best predictions over the range of operating conditions and system parameters, are shown here. The most robust model employs the Wen and Yu[15] drag force relation, the Peirano and Leckner[20] solid stress model, and the FET closure for the interaction between the gas and particle velocity fluctuations along with the Sinclair and Mallo[12] closure for the cross-correlation.

Since the experimental data by Tsuji et al.[21] is the most widely cited, the data sets for 243 μm and 500 μm are chosen here as a standard by which all the previously published models, as well as the present model, will be evaluated. However, all of the models have been evaluated against all the experimental data summarized in Table 8, and it is observed that the model utilizing the combination of Wen and Yu[15] drag force relation, the Peirano and Leckner[20] solid stress model, and the FET closure compare more favorably to the data than the other models. The values for the coefficient of restitution of particle-particle/particle-wall collisions and the specularity factor are the same as those given in Bolio et al.[2] and are approximately similar to the values employed in the other published gas-solid flow models.

Results and Discussion

From the simulations, profiles of the gas and solid mean velocities V_{gz} and V_{sz}, along with the profiles of the gas turbulent kinetic energy k and the granular temperature T are obtained. Since experimental data report values for the axial solid velocity fluctuations v_{sz}', these values need to be extracted from the predicted granular temperature T. To convert T to v_{sz}', isotropic solid velocity fluctuations are assumed. Measurements of axial and radial solid velocity fluctuations show that this assumption is a reasonable one for dilute gas-solid flow[32]

$$v_{sz}' = \sqrt{T} \tag{29}$$

For the gas velocity fluctuations, Sheen et al.[23] has shown that the gas turbulence is not isotropic in pipe flows. Consequently, it is assumed that the radial and azimuthal fluctuations in velocity v_{gr}' and $v_{g\theta}'$ respectively, are approximately half of the axial velocity fluctuations[23]

$$v_{gr}' = v_{g\theta}' = \frac{v_{gz}'}{2} \tag{30}$$

which results in

$$v_{gz}' = \sqrt{k} \tag{31}$$

Figures 3 to 6 compare the predicted profiles of the new model (which incorporates the Wen and Yu[15] drag force, the Peirano and Leckner[20] solids stress, the new FET model for the interaction between the gas and particle velocity fluctuations, and the Sinclair and Mallo[12] model for the solid-gas velocity cross-correlation) to the experimental data of Tsuji et al.[21] Figures 7 and 8 compare the predicted profiles from the same model to the Jones et al.[22] and Sheen et al.[23] data, respectively. In all of these predictions, when the Stokes number ($ST = \frac{d^2 V_{avg} \rho_s}{18 \mu_g (2R)}$) is less than 100, the particle relaxation time scale τ_D is used as the time scale for the fluctuation energy transfer. When ST is less than 100, the mechanism of the fluid being pulled along by the particles causes the transfer of the fluctuation energy. On the other hand, when ST is greater than 100, the particle collision time scale τ_c is used because the change in direction of the individual solid particles and the corresponding disturbance in the particle wake are responsible for the transfer of the fluctuation energy. Finally, if $Re_p > 150$ (large particles with large relative velocity), E_w is activated. When Re_p is greater than 150, the turbulent boundary layer detaches from the particle surface and vortices are generated in the wake of the solid particles, enhancing gas-phase turbulence. Table 9 summarizes the time scales used by the FET model for the various experimental data (detailed in Table 8).

Table 10. Percentage Error in Predicted Gas Velocity Fluctuations Using the Various Combinations of Different Interaction Terms and Velocity Cross Correlations

		d = 243 μm			d = 500 μm			
Interaction Term	Cross Correlation	m=0.5	m=1.3	m=3.2	m=0.7	m=1.3	m=3.4	Average Error%
FET Eqs. 25 and 26	Sinclair and Mallo[12]	3.65	9.14	5.10	1.03	4.30	2.58	4.30
TVBA Eqs. 4 and 5	Louge et al.[1]	5.49	8.97	17.57	4.11	6.84	16.70	9.95
TVBA Eqs. 4 and 5	Koch and Sangani[9]	6.53	16.37	26.99	5.15	9.40	25.82	15.04
TVBA Eqs. 4 and 5	Wylie et al.[11]	6.53	16.37	27.00	5.15	9.40	25.83	15.05
TVBA Eqs. 4 and 5	Simonin[3]	6.47	15.59	18.69	5.14	9.34	24.36	13.27
TVBA Eqs. 4 and 5	Sinclair and Mallo[12]	3.03	11.22	11.42	1.44	3.02	7.86	6.33

Table 11. Percentage Error in Predicted Solid Velocity Fluctuations Using the Various Combinations of Different Interaction Terms and Velocity Cross Correlations

Interaction term	Cross Correlation	$d = 243$ μm			Average error%
		m=0.5	m=1.3	m=3.2	
FET Eqs. 25 and 26	Sinclair and Mallo[12]	4.25	8.05	4.29	5.53
TVBA Eqs. 4 and 5	Louge et al.[1]	9.41	14.29	8.41	10.70
TVBA Eqs. 4 and 5	Koch and Sangani[9]	10.29	15.29	9.56	11.72
TVBA Eqs. 4 and 5	Wylie et al.[12]	10.29	15.29	9.56	11.72
TVBA Eqs. 4 and 5	Simonin[3]	10.22	15.24	9.32	11.59
TVBA Eqs. 4 and 5	Sinclair and Mallo[12]	2.87	8.42	3.93	5.07

Overall, the simulation results for the mean gas and solid velocities, as well as the fluctuating gas and solid velocities, favorably match the experimental data with this proposed model. The predictions for gas-solid flow shown in Figure 6 for 2.80 mm particles are not as good as the other cases. This discrepancy is likely due to an inadequate description for vortex shedding with such large particles.

Comparing the various models for interaction terms and cross-correlations

The different models for the interaction terms are compared using the gas-phase turbulence and granular temperature data for the 243 μm and 500 μm particles of Tsuji et al.[21] These experimental data are used as the standard for uniformly comparing model predictions since most (all but Zhang and Reese[14]) of the other closure models do not predict gas-phase turbulence enhancement in the presence of large particles (1.42 mm and 2.78 mm).

To focus this comparison on the effect of the model predictions from the various descriptions for interaction terms and the cross-correlation, the same drag force relation, Wen and Yu,[15] and the same solid-phase stress, Perino and Leckner,[20] are used in generating the model predictions. Furthermore, only the gas fluctuation velocity (v_{gz}') and the solid fluctuation velocity (v_{sz}') are compared, as variations in the predicted mean gas and solid velocity profiles are negligible.

To quantify the comparisons between the model predictions, a percentage error, reflecting the deviation between the measured value and prediction is calculated, for the three different solids loadings with the two different particle sizes. The percentage error for the gas phase is defined as

$$\%\text{error} = \frac{\sqrt{\sum_j \left(v'^{\text{expt}}_{gzj} - v'^{\text{sim}}_{gzj}\right)^2}}{\sum_j v'^{\text{expt}}_{gzj}} \times 100 \qquad (32)$$

where v'^{expt}_{gzj} is the jth experimental value of the fluctuating gas velocity and v'^{sim}_{gzj} is the predicted value of the fluctuating gas velocity at the same radial position r at its corresponding jth experimental value. The percentage error for the solid fluctuating velocity predictions is similarly defined for the solid phase. These error values have been reported in Tables 10 and 11 and show that most models are able to capture the very dilute mass loading flow cases, but fail to aptly predict the cases with larger mass loading.

Figure 9(a) compares the magnitude of the βk_{sg} (where β is calculated from the Wen and Yu[15] drag correlation and k_{sg} is calculated from the various cross-correlations) for the various combinations of interaction terms and the cross-correlation models for the Tsuji et al.[21] case of 243 μm particles with a solids loading of 3.2. Similarly, I_k (Eq. 4), along with the generation $(1-v)\mu^T\left(\frac{\partial V_{gz}}{\partial r}\right)^2$ (calculated using FET model only), are compared in Figure 9(b), and I_T (Eq. 5), along with the rate of granular energy dissipation ($\gamma = \frac{48}{\sqrt{\pi}}\eta(1-\eta)g_0 v^2 \frac{\rho_s}{d} T^{3/2}$, calculated again using FET model only), are compared in Figure 9(c).

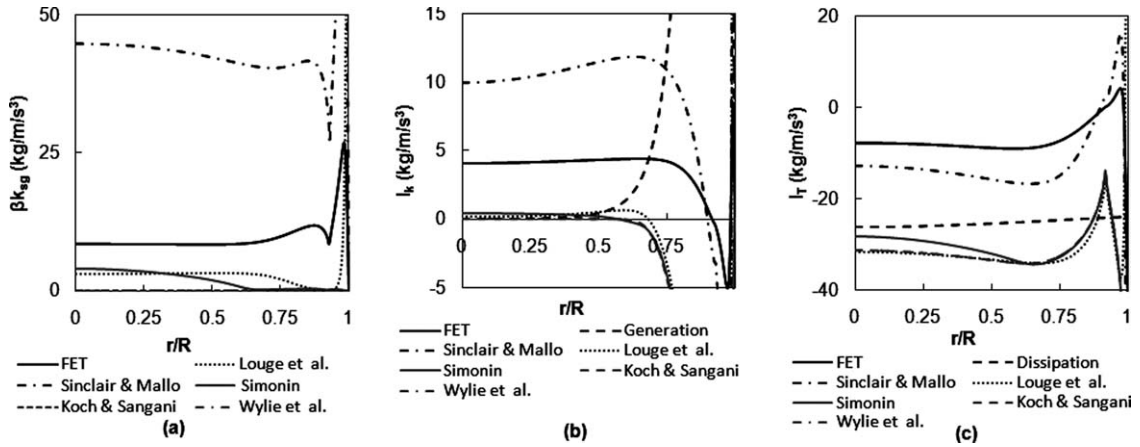

Figure 9. Comparing the magnitudes of (a) βk_{sf}, (b) I_k, and (c) I_T for the various interaction term models for the case of 243 μm particles with $m = 3.2$.[21]

Table 12. Percentage Error in Predicted Gas Velocity Fluctuations Using the Various Drag Relations

Models	$d = 243$ μm			$d = 500$ μm			Average error%
	$m = 0.5$	$m = 1.3$	$m = 3.2$	$m = 0.7$	$m = 1.3$	$m = 3.4$	
Wen and Yu[15]	3.65	9.14	5.10	1.03	4.30	2.58	4.30
Hill et al.[16,17]	3.76	10.25	8.41	0.88	4.00	4.12	5.24
Syamlal and O'Brien[18]	3.65	9.05	4.34	1.01	4.22	2.30	4.10

From Figure 9(b), it is observed that the generation is very small at the core of the pipe and sharply rises toward the wall. For the FET model, the I_k term dominates at the core of the pipe, and the remaining two terms, the generation and the dissipation ε [not shown in Figure 9(b)], play an important role near the wall of the pipe. Since I_k dominates at the core of the pipe, the gas-phase turbulence k largely depends on the interaction term. While, at the wall, the gas-phase turbulence depends on the generation and the dissipation.

Further, from Figure 9(c), the FET model predicts that I_T will be negative and all three terms in the granular temperature equation, granular temperature generation [not shown Figure 9(c)], dissipation, and interaction play equally important roles throughout the pipe. No one term dominates at any radial position.

In cases in which the Louge et al.,[1] Koch and Sangani,[9] and Wylie et al.[11] cross-correlation models (these models use TVBA for I_k and I_T) are used, the error in predicting the gas-phase turbulence profile (Table 10) increases as the mass loading increases, especially at the core of the pipe. This result is because the magnitude βk_{sg} in Eq. 4 is underestimated, and consequently, I_k is small compared to the gas-phase generation [Figure 9(b)], even at the center of the pipe. Additionally, the I_T values estimated form Louge et al.,[1] Koch and Sangani,[9] and Wylie et al.[11] models are more negative than what is predicted from the FET model resulting in poorer model predictions (Tables 10 and 11). All the cross-correlation models that contain a square of the relative velocity $\left(V_{gz} - V_{sz}\right)^2$ term (Table 6) produce a profile for k_{sg} that increase rapidly near the wall as the relative velocity between the gas and solid phases is very large. However, βk_{sg} must be zero at the wall (as $k_{sg} = 0$, no slip condition).

Although the Simonin[3] cross-correlation model yields values for I_k which dominate the k-equation at the pipe center, the predictions of shape and magnitude of the fluctuation gas velocity are not as good as those obtained from the FET model (which uses the Sinclair and Mallo[12] model for cross-correlation), especially for higher mass loading. These poor predictions are because the Simonin[3] model predicts too much turbulence damping since the I_k values obtained from it are smaller than those from the FET model [Figure 9(b)]. On the other hand, the Sinclair and Mallo[12] closure (using TVBA for I_k and I_T) predicts the order of magnitude of k and T profiles well, but fails to predict the shape of the k profile correctly.

As mentioned earlier, the code was unable to reproduce the results of Zhang and Reese[14] even after consultation with the authors. Stable model solutions could not be obtained for the Tsuji et al.[21] 243 μm particles, and the model predictions for the 500 μm particles were poor. The additional generation term $\beta(1-v)\left(V_{gz} - V_{sz}\right)^2$ (Eq. 14) produces values for I_k which are up to two orders of magnitude larger than the typical range and yields an unrealistically large increase in the gas-phase turbulence resulting in unstable solutions in some cases.

Based on Figure 9(b,c), all the models predict I_k to be positive, which implies a net generation of gas turbulence at the core of the pipe, while I_T is negative which implies a net dissipation of granular temperature. The interaction term I_T in the granular temperature equation behaves as dissipation, taking energy from the solid phase and transferring it to the fluid phase resulting in a generation of gas-phase turbulence. This idea goes well with the concept of the fluctuation energy transfer mechanism.

It is observed experimentally that for small particles ($d <$ 300 μm or $40 < ST < 100$), the solid velocity fluctuations are larger than the fluid velocity fluctuations at the core of the pipe. Furthermore, for such particles, if the solids loading increases, the magnitude of the solid velocity fluctuations reduces due to enhanced particle-particle collisions and larger inelastic dissipation. The reduction in the granular temperature T (solid velocity fluctuations) tends to further dampen the gas-phase turbulence through the energy coupling terms (I_k, I_T). Hence, higher the mass loading, more is the gas-phase turbulence dampening [Figure 3(b,c)]. Flow predictions employing

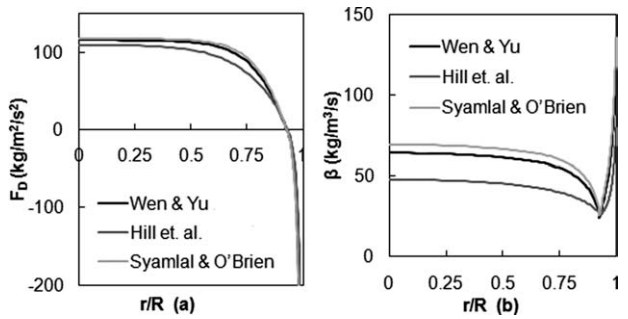

Figure 10. Comparing the magnitudes of (a) F_D and (b) β for the various drag models for the case of 243 μm particles with $m = 3.2$.[21]

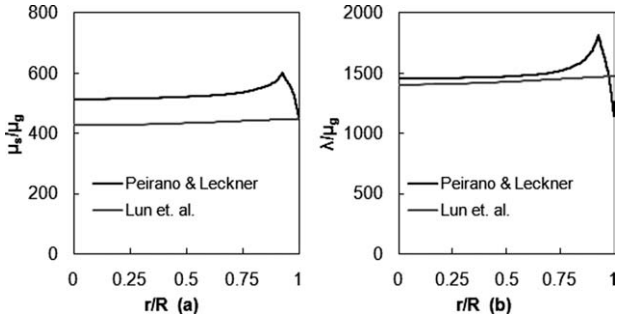

Figure 11. Comparing the magnitudes of (a) μ_s/μ_g and (b) λ/μ_g for the various solid stress models for the case of 243 μm particles with $m = 3.2$.[21]

Table 13. Percentage Error in Predicted Gas Velocity Fluctuations Using the Various Solid Stress Closures

Models	$d = 243$ μm			$d = 500$ μm			Average error%
	$m = 0.5$	$m = 1.3$	$m = 3.2$	$m = 0.7$	$m = 1.3$	$m = 3.4$	
Peirano and Leckner[20]	3.65	9.14	5.10	1.03	4.30	2.58	4.30
Lun et al.[19]	3.77	9.53	4.97	1.03	4.28	2.71	4.38

the FET interaction model are able to reproduce these experimental observations and trends very well.

For the case of very large particles [$d > 800$ μm or $Re_p > 150$, Figures 5(b) and 6] with a large degree of slip (V_{gz}-V_{sz}), the vortex shedding E_w overpowers the effect of the interaction term I_k in the k-equation which results in large gas-phase turbulence. Also, as the solids mass loading increases, more vortex shedding takes place, which further enhances the gas-phase turbulence. The predicted fluid velocity fluctuations employing the FET model are greater than the solid velocity fluctuations ($2k > 3T$) resulting in a net dissipation of the fluid-phase velocity fluctuations and a net generation for the solid phase. Thus, a counter effect is seen in these cases with larger particles in which increases in solid mass loading reduces T by increasing γ, but this effect is offset by the increase in I_T. Overall, the granular temperature T slowly increases as the solids mass loading increases. Unfortunately, solid velocity fluctuation data are not available for these larger particles to validate these model predictions.

The intermediate particle sizes [300 μm $< d <$ 800 μm or $ST > 100$ and $Re_p < 150$, Figure 4(b)] display flow behavior between the two extremes, where the gas turbulence is enhanced at the core of the pipe but dampened at the wall as compared to single-phase flow. Also, the simulations incorporating the FET interaction term model predict that the solid velocity fluctuations are greater than the fluid fluctuations at low solid mass loadings, but the fluid fluctuations become greater than those of the solid as the mass loading increases. Again, there are no solid fluctuation data to validate these model predictions for the solid-phase fluctuations, but the model favorably matches the experimental gas-phase fluctuation data.

All of these predicted qualitative trends obtained by using the FET interaction term model, along with the Sinclair and Mallow[12] cross-correlation, are in line with the well-known work of Gore and Crowe.[5] These authors suggested that for small particles, drag is responsible for the turbulence transfer between the phases and turbulence damping. In the FET model, the drag time scale τ_D is used as the time scale for energy transfer for small particles. Furthermore, Hestroni[6] showed that particles with intermediate Re_p display in-between behavior (i.e., gas-phase turbulence enhancement in the core of the pipe and dampening at the wall). In the FET model this behavior occurs when τ_c is the time scale, but vortex shedding is not activated (i.e., $ST > 100$ but $Re_p <$ 150). Hestroni[6] also showed that for very large Re_p, vortex shedding is responsible for enhanced turbulence as is seen in the cases in which $Re_p > 150$. The vortex shedding, in this study, is described using E_w.

The FET model predictions for particle sizes ranging from 70 to 3000 μm with a wide range of mass loadings compare very well with the experimental data. Hence, the FET model along with the Sinclair and Mallo[12] cross-correlation is recommended over the other previously proposed closure models for the interaction terms and the solid-gas fluctuating velocity cross-correlation.

Comparing the various models for drag terms

Flow predictions using different drag force relations are compared in Table 12, which provides the percentage error values of the predictions from the experimental data. To compare the different drag relations, the FET interaction model, along with the Sinclair and Mallo[12] cross-correlation and the Perino and Leckner[20] solid stress model were employed. Figure 10 shows that the magnitude of the drag force based on the Wen and Yu[15] and Syamlal and O'Brien[18] models for the case of 243 μm particles and $m = 3.2$ of Tsuji et al.[21] are very similar. The Hill et al.[16,17] drag relation predicts a drag force magnitude slightly smaller than the other two models. The percentage error values in Table 12 for the Hill et al.[16,17] drag relation are slightly larger than the other two models, suggesting that the Hill et al.[16,17] drag relation may under predict the drag coefficient β and thereby under predict the drag force.

Hadinoto and Curtis[10] studied the effect of the various drag relations for particles with low inertia on two-phase flow predictions. They observed some influence on the predictions of slip velocity due to changes in the drag model; however, no such effect is seen in this study since the particles studied herein have large inertia. Hence, the effect of the choice of the drag model is not that significant. Since the predicted flow profiles found by changing the drag models are similar, the Wen and Yu[15] model, a robust and widely used closure, is recommended for the case of dilute, turbulent, gas-solid flow models.

Comparing the various models for solid stress terms

Figure 11 compares the magnitude of the solid phase viscosity μ_s and solid phase conductivity λ using the Lun et al.[19] and the Peirano and Leckner[20] solid stress closures for the case of 243 μm particles and $m = 3.2$ in the experiments of Tsuji et al.[21] The FET interaction model and the Wen and Yu[15] drag relation were employed in this comparison. Both the solid viscosity μ_s and conductivity λ values, as predicted by the Lun et al.[19] model, are insensitive to the radial position r. Both the μ_s and λ are primarily functions of the granular temperature, which is essentially constant over the pipe cross-section. In contrast, the predicted solid viscosity and conductivity from the Peirano and Leckner[20] solid stress closure exhibit some dependency on the radial position r, as this solid stress model incorporates a direct effect of the fluid on the μ_s and λ values. Table 13 shows that the two solid stress closures produce similar error in the model predictions from the experimental data. Furthermore, the detailed shape of the mean and fluctuating solid and gas profiles obtained from the two solid stress closures are hardly different. Since the Peirano and Leckner[20] solid stress closure directly incorporates fluid effects, it is chosen over the Lun et al.[19] solid stress closure.

Conclusion

Experimental data for fully developed profiles of pneumatically conveyed solid particles in a vertical pipe (Tsuji, personal communication)[21] have been available in the literature for more than 20 years. Many authors have proposed Eulerian based, dilute turbulent gas-solid flow models incorporating particle-particle interactions using a two-equation k-ε model to describe gas-phase turbulence[2–4,14] to simulate these data. These Eulerian models have used various combinations of relations of drag, solid-phase stress, and fluctuating interaction terms to successfully predict for the gas-solid flows the mean velocities. Unfortunately these models consistently under predict the gas turbulence and granular temperature. In this study, the work of Bolio et al.[2] is advanced to include a new closure relation for the fluctuating velocity interaction.

The proposed new model (FET model along with Sinclair and Mallo,[12] cross-correlation) for the interaction term is formulated using an analogy with heat transfer. The time scales for the FET model depend on the Stokes number (ST) while activation of vortex shedding depends on Re_p (Table 7). If $ST < 100$, particle drag is responsible for the energy transfer and if $ST > 100$, then particle collisions are responsible for energy transfer. These observations are consistent with the findings of Gore and Crowe[5] and Hestroni.[6]

The proposed new fluctuating interaction model, along with the Wen and Yu[15] drag relation, the Peirano and Leckner[20] solid stress closure which includes fluid effects, is evaluated against several benchmark experimental data sets. The new model predicts the mean velocity profiles and also the fluctuations velocity profiles of gas and solid for both small and large particles. For particles with $Re_p > 150$ vortex shedding is included in this model. It is also observed that the fluctuating interaction terms strongly influence the magnitude of gas turbulence away from the wall. Near the wall, turbulence generation and dissipation dominate over the fluctuating interaction term. In contrast, the predicted profiles are not sensitive to the choice of drag model or the solid-stress closure.

Acknowledgments

This work was supported by the National Science Foundation under Grant No. 0749481 and by the CPaSS industry members.

Notation

A_{ht} = area of heat transfer, L^2
A_{PL}, B_{PL}, C_{PL}, D_{PL} = coefficients based on e for Peirano and Leckner,[20] -
A_{SO}, B_{SO} = parameter based on v for Syamlal and O'Brien model, -
C_D = friction factor, -
c_{T1}, c_{T2}, c_{T3}, c_μ = constants in k-ε model, -
C_w = coefficient for turbulence generation by vortex shedding, -
c_β = parameter based on angle between flow direction and slip velocities, -
d = particle diameter, L^1
e = particle-particle coefficient of restitution, -
e_w = particle-wall coefficient of restitution, -
E_w = turbulence generation by vortex shedding, $M^1L^{-1}T^{-3}$
F, F_0, F_1, F_2, F_3 = dimensionless functions based on Re_p and v for Hill et al.[16,17] model, -
F_D = drag force per unit volume, $M^1L^{-2}T^{-2}$
f_D = the fluctuating drag force per unit volume, $M^1L^{-2}T^{-2}$
f_{T1}, f_{T2}, f_μ = coefficients in k-ε model, -
g = gravitational acceleration, L^1T^{-2}
g_0 = radial distribution coefficient, -
G_{1k}, G_{1c}, G_{2k}, G_{2c}, G_{3k}, G_{3c} = dimensionless functions based on e and T, -
h = heat transfer coefficient, $M^1T^{-2}\tau^{-1}$
I_k = interaction terms in the k equation, $M^1L^{-1}T^{-3}$
I_T = interaction terms in the T equation, $M^1L^{-1}T^{-3}$
k = gas turbulence kinetic energy, L^2T^{-2}
k_{fb} = coefficient based on v, -
k_{sg} = cross-correlation between gas-phase and solid-phase fluctuating velocities, L^2T^{-2}
m = mass loading, -
p = pressure, $M^1L^{-1}T^{-2}$
q_{PT} = granular energy flux, M^1T^{-3}
r, z,θ = coordinate system, L^1
R = radius of pipe, L^1
Re = Reynolds number of flow, -
Re_p = particle Reynolds number, -
Re_T = Reynolds number based on $\sqrt{T}$, -
R_T = turbulent Reynolds number, -
ST = Stokes number, -
T = granular temperature, L^2T^{-2}
t = time, T^1
T_f = real temperature of a fluid, τ^1
U_τ = friction velocity, L^1T^{-1}
v_g' = fluctuating gas—phase velocity, L^1T^{-1}
V_g = mean gas—phase velocity vector, L^1T^{-1}
V_{rm} = dimensionless velocity based on Re_p and v for Syamlal and O'Brien model, -
v_s' = fluctuating solid—phase velocity, L^1T^{-1}
V_s = mean solid—phase velocity vector, L^1T^{-1}
w_{HLK} = dimensionless parameter based on Re_p and v for Hill et al.[17,18] model, -
y^+ = dimensionless distance from the wall, -

Greek letters

β = drag coefficient, $M^1L^{-3}T^{-1}$
β' = FET coefficient, $M^1L^{-3}T^{-1}$
γ = dissipation rate of granular energy, $M^1L^{-1}T^{-3}$
ε = dissipation of gas turbulence, L^2T^{-3}
θ' = angle between flow direction and slip velocities, -
λ = conductivity of granular temperature modified by inelastic collisions, $M^1L^{-1}T^{-1}$
λ' = conductivity of granular temperature, $M^1L^{-1}T^{-1}$
λ_{mfp} = particle mean free path, L^1
μ_b = bulk solid-phase viscosity, $M^1L^{-1}T^{-1}$
μ_{eg} = gas-phase viscosity modified by particles, $M^1L^{-1}T^{-1}$
μ_g = gas-phase viscosity, $M^1L^{-1}T^{-1}$
μ_s = solid-phase viscosity modified by inelastic collisions, $M^1L^{-1}T^{-1}$
μ_s' = solid-phase viscosity, $M^1L^{-1}T^{-1}$
μ_T = turbulent gas-phase viscosity, $M^1L^{-1}T^{-1}$
μ_t = turbulent gas-phase viscosity for vortex shedding, $M^1L^{-1}T^{-1}$
v = solid volume fraction, -
v_0 = random closest packing, -
ξ_r = parameter based on relative velocity and k, -
ρ_g = gas phase density, M^1L^{-3}
ρ_s = solid phase density, M^1L^{-3}
σ = solid-phase shear stress tensor, $M^1L^{-1}T^{-2}$
σ^c = collisional component of solid- phase shear stress tensor, $M^1L^{-1}T^{-2}$
σ_k, σ_ε = constants in k-ε model, -
σ^k = kinetic component of solid-phase shear stress tensor, $M^1L^{-1}T^{-2}$

τ = fluid stress tensor, $M^1L^{-1}T^{-2}$
τ_c = time between particle collisions, T^1
τ_D = particle relaxation time scale, T^1
τ_e = eddy time scale, T^1
τ_L = Lagrangian time scale, T^1
τ_* = time scale for FET model, T^1
τ^{TURB} = turbulent component of gas-phase stress, $M^1L^{-1}T^{-2}$
χ = ratio of mass of solid in a unit volume to the mass of fluid in the same volume, -
Ψ = function based on v, -
Ψ', Ψ'' = functions based on v, Re_p, Re_T, -
ω = damping function, -
Φ = specularity, -
η = parameter based on e, -
η_t = ratio of Lagrangian time scale to particle relaxation time scale, -

Subscripts

i,j = indices
r, z, θ = coordinate system
s = solid phase
g = gas phase

Literature Cited

1. Louge M, Mastorakos E, Jenkins J. The role of particle collisions in pneumatic transport. *J Fluid Mech*. 1991;231:345–359.
2. Bolio E, Yasuna J, Sinclair J. Dilute turbulent gas-solid flow in risers with particle-particle interaction. *AIChE J*. 1995;41:1375–1388.
3. Simonin O. *Continuum modeling of dispersed two-phase flow*. In: *Combustion and turbulence in two phase flow. Von Karman Institute of Fluid Dynamics, Lecture Series*, Rhode-Saint-Genèse, Belgium, 1996.
4. Benviades A, van Wachen B. Numerical simulation and validation of dilute turbulent gas-particle flow with inelastic collisions and turbulence modulation. *Powder Technol*. 2008;182:294–306.
5. Gore R, Crowe C. Effect of particle size on modulating turbulent intensity. *Int J Multiphase Flow*. 1989;15:279–285.
6. Hestroni G. Particles-turbulence interaction. *Int J Multiphase Flow*. 1989;15:735–746.
7. Koch D. Kinetic theory for a monodispersed gas-solid suspension. *Phys fluids*. 1990;2:1711–1722.
8. Igci Y, Andrew IV A, Sundaresan S, Pannala S, O'Brien T. Filtered two-fluid models for fluidized gas-particle suspensions. *AIChE J*. 2008;54:1431–1448.
9. Koch D, Sangani A. Particle pressure and marginal stability limits for homogeneous monodisperse gas-fluidized bed: kinetic theory and numerical simulations. *J Fluid Mech*. 1999;400:229–263.
10. Hadinoto K, Curtis J. Numerical simulation of turbulent particle-laden flowa with significant fluid to particle inertia ratio. *Ind Eng Chem Res*. 2009;48:5874–5884.
11. Wylie J, Koch D, Ladd A. Rhelogy of suspension with high particle inertia and moderate fluid inertia. *J Fluid Mech*. 2003;480:95–118.
12. Sinclair J, Mallo T. *Describing Particle-Turbulence Interaction in a Two-Fluid Modeling Framework, Vol. 4*. ASME Fluids Engineering Division Summer Meeting. New York: ASME Press, 1998:7–14.
13. Crowe C. On models for turbulence modulation in fluid-particle flows. *Int J Multiphase Flow*. 2000;26:710–727.
14. Zhang Y, Reese J. Gas turbulence modulation in a two-fluid model for gas-solid flows. *AIChE J*. 2003;49:3048–3065.
15. Wen C, Yu Y. Mechanics of fluidization. *Chem Eng Progr Symp Ser*. 1966;62:100–111.
16. Hill R, Koch D, Ladd J. The first effects of fluid inertia on flows in ordered and random arrays of spheres. *J Fluid Mech*. 2001;448:213–241.
17. Hill R, Koch D, Ladd J. Moderate-Reynolds-number flows in ordered and random arrays of spheres. *J Fluid Mech*. 2001;448:243–278.
18. Benyahia S, Syamlal M, O'Brien T. Summary of MFIX equations. 2007. Available at www.mfix.org: http://www.mfix.org/documentation/MfixEquations2005–4-3.pdf.
19. Lun C, Savage S, Jeffery D, Chepurniy N. Kinetic theories for granular flow: inelastic particles in couette flow and slightly inelastic particles in general flow field. *J Fluid Mech*. 1984;140:223–256.
20. Peirano E, Leckner B. Fundamentals of turbulent gas-solid applied to circulating fluidized bed combustion. *Progr Energy Combut Sci*. 1998;24:259–296.
21. Tsuji Y, Morikawa Y, Shiomi H. LDV measurements of air-solid two-phase flow in a vertical pipe. *J Fluid Mech*. 1984;139: 417–434.
22. Jones E, Yurteri C, Sinclair J. Effect of mass loading on gas-solids motion and particle segregation patterns. *Handbook Powder Technol*. 2001;10:843–849.
23. Sheen H, Chaing Y, Chaing Y. Two dimensional measurements of flow structure in a two phase vertical pipe flow. *Proc Natl Sci Council, Republic of China (A)*. 1993;17:200–213.
24. Lee S, Durst F. On the motions of particles in turbulent duct flow. *Int J Multiphase Flow*. 1982;8:125–146.
25. Benyahia S. Gas/solids turbulence models implemented in MFIX. 2005; Available at www.mfix.org: https://www.mfix.org/documentation/Simonin_Ahmadi_Models.pdf.
26. Batchelor G, Green, J. The determination of bulk stress in a suspension of spherical particle to order of c2. *J Fluid Mech*. 1972;56: 401–427.
27. Benyahia S, Syamlal M, O'Brien T. Extension of Hill-Koch-Ladd drag correlation over all ranges of Reynolds number and solid volume fraction. *Powder Technol*. 2006;162:166–174.
28. Lun C. Numerical simulation of dilute turbulent gas-solid flows. *Int J Multiphase Flow*. 2000;26:1707–1736.
29. Johnson P, Jackson R. Frictional-collisional constitutive relations for granular materials with applications to plane shearing. *J Fluid Mech*. 1987;176:67–93.
30. Benyahia S, Syamlal M, O'Brien T. Study of the ability of multiphase continuum models to predict core-annulus flow. *AIChE J*. 2007;53:2549–2568.
31. Patankar S, Spadling D. *Heat and Mass Transfer in Boundary Layers*. London: Morgan-Grampain Press, 1967.
32. Jones E. An experimental investigation of particle size distribution effect in dilute phase gas-solid flow. PhD thesis, Perdue University, 2001.

Manuscript received Feb. 8, 2011, and revision received Apr. 28, 2011.